

Effects of B_2O_3 and TiO_2 on crystallization behavior of some slags in Al_2O_3 - CaO - MgO - Na_2O - SiO_2 system

Qifeng SHU^{1),2)}, Zhen WANG¹⁾, Jeferson L. KLUG^{2),3)}, Kuochih CHOU¹⁾ and Piotr R. SCHELLER²⁾

- 1) School of metallurgical and ecological engineering, University of Science and Technology Beijing, Beijing 100083, China
- 2) Institute of iron and steel technology, Freiberg university of mining and technology, D-09596, Freiberg, Germany
- 3) Federal University of Rio Grande do Sul, Rio Grande do Sul, Porto Alegre 90040-060, Brazil

Abstract: Nowadays, there are increasing demands for developing mould fluxes without fluoride due to environmental concerns. Slag bearing titanium oxide and/or boron oxide proved to be promising substitute for traditional mould fluxes with fluoride. In the present work, Crystallization behaviors of some slags in Al_2O_3 - CaO - MgO - Na_2O - SiO_2 - B_2O_3 - TiO_2 system were investigated using Single Hot Thermocouple Technique (SHTT), Differential Thermal Analysis (DTA) and X-ray diffraction (XRD) techniques. It was found that the liquidus temperature of slag decreases with increases of B_2O_3 content. The XRD analysis on the crystallized samples shows that crystallization products are perovskite, gehlenite and wollastonite. Time- Temperature- Transformation diagrams (TTT) for various slags have been constructed using SHTT technique. It was found that B_2O_3 can significantly increase the incubation time for crystallization of slags. The incubation time for crystallization of slags decreases with increase of titanium oxide content from 5% to 10%. The morphology of crystals was also investigated using SHTT technique. At higher temperature, dendrites and columnar crystal tend to form and grow with time progress, while at lower temperature, small crystals appear and the amount of crystal increase with time increasing.

Keywords: Non-fluoride mould fluxes, crystallization, single hot thermocouple, DTA

1. Introduction

During casting of steel, mould fluxes are placed on top of steel to protect steel from oxidation[1]. Several top layers of mould fluxes are formed by heating of steel, and liquid fluxes would infiltrate into gap between steel and mould. When liquid fluxes contact the water cooling copper mould, glassy layer forms due to fast cooling. Crystallization could take place in hotter regions of glassy layer. The thickness of Glassy and crystalline layer depend on slag chemistry and different conditions of cooling. Heat transfer between mould and steel shell is very important for eliminating the surface defects such as longitude cracking. Crystallization of mould slag is a very important factor to control heat transfer between mould and steel.

Traditional mould fluxes consist of certain amounts of fluoride in order to decrease of melting temperature, viscosity and provide some crystals (cuspidine) in solid slag layer. However, the use of fluoride in mould fluxes would bring important environmental problem in casting plant[2]. Fluorine is harmful to human health. Gaseous HF, SiF_4 , NaF could emit into atmosphere during casting. Fluoride in mould slag could be leached into ground water in plant. Therefore, in recent years, many researchers were dedicated to develop fluoride-free mould fluxes to eliminate the emission of fluorine in steel casting [3-5]. Fox et al. [3] studied fluoride-free fluxes with B_2O_3 and Na_2O as alternative

substitutes for CaF_2 in billet fluxes, and they tested new flux successful in a plant trial on a continuous casting plant. Nakada et al [4] investigated the crystallization of slags in $\text{CaO-TiO}_2\text{-SiO}_2$ system as a candidate for fluorine free mould flux. They proposed that CaSiTiO_5 could be a good substitute for cuspidine in commercial mould fluxes due to rapid crystallization in slag film. It could be concluded that slag bearing B_2O_3 and TiO_2 has receive strong attention as a candidate for fluoride-free mould fluxes.

In this work, crystallization behaviors of some slags in $\text{Al}_2\text{O}_3\text{-CaO-MgO-Na}_2\text{O-SiO}_2\text{-B}_2\text{O}_3\text{-TiO}_2$ system were investigated using Single Hot Thermocouple Technique (SHTT)[6-8], Differential Thermal Analysis (DTA) and X-ray diffraction (XRD) technique. Characteristic temperatures (liquidus, solidus, glass transformation and crystallization temperature) of slag samples were determined by DTA. The crystallization products were analyzed using XRD. Time-Temperature-Transformation diagram were constructed using SHTT technique. The morphologies of crystallites formed were also investigated using SHTT.

2. Experimental

2.1 Sample preparation

Reagent grade MgO , Al_2O_3 , Na_2CO_3 , CaO , TiO_2 , SiO_2 and H_3BO_3 were adopted as raw material to produce slags. Na_2CO_3 and H_3BO_3 were substitutes for Na_2O and B_2O_3 due to its stability in air. The reagent powders were mixed well in agate mortar and melted in platinum crucible with a MoSi_2 box furnace. After melting, slags were quenched in water to form cullet. The slag samples were testified as glass by XRD.

The compositions (wt. %) of the slag samples investigated in the present work were shown in Table 1.

Table 1 Chemical composition of slag investigated (mass%)

No.	CaO	SiO ₂	Al ₂ O ₃	MgO	Na ₂ O	TiO ₂	B ₂ O ₃
1	W(CaO)/w(SiO ₂)=1		7	2	10	5	0
2			7	2	10	5	5
3			7	2	10	5	10
4			7	2	10	10	5
5			7	2	10	5	3
6			7	2	10	3	5

2.2 DTA analysis

DTA analyses were performed at Netzsch STA-449C thermal analyzer in argon atmosphere. The samples were heated from room temperature to 1473K with a heating rate of 10°C/min and DTA signals were recorded simultaneously. Al_2O_3 was taken as reference material.

2.3 XRD analyses

Crystallization products were analysed by XRD. The glassy slags were treated at peak temperature determined by DTA analyses for 2 hours for crystallization. The products were crushed and ground to subject to XRD. XRD analyses were performed at M21XRHF22 (Mac Science, Japan) X-ray diffract meter.

2.4 SHTT measurement

A SHTT setup was constructed in the institute of iron and steel technology, TU Bergakademia Freiberg [8]. A

schematic view could be shown in Fig.1. The facility consists of a vacuum chamber with two water-cooled inserts left and right, both of which hold a thermocouple with 0.5 mm diameter at their tip. The equipment makes it possible to measure the temperature with a thermocouple while it is heated simultaneously. This is managed by a complex electronic circuit which separates both electronic signals. The heating and cooling of the thermocouples are controlled by a PID controller independently. The temperature measurement is calibrated by measuring the melting point of pure salts as Na_2SO_4 , K_2SO_4 and CaF_2 . The maximum working temperature of the system is 1700°C . Usually the sample on the thermocouples could be observed down to 900°C , due to light emission at high temperature. With an additional light source from below transparent samples can be observed down to room temperature. Maximum cooling rate can be more than 50K/s when free cooling is applied.

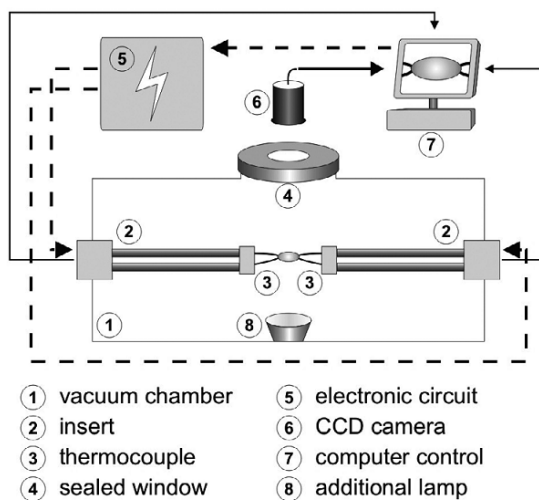


Fig. 1 Schema of Single/double high temperature thermocouple setup [8]

To determine the TTT diagram for slag samples, the samples are heated to high temperature (1300°C) and held for several minutes to ensure complete melting and homogenize its composition and temperature. After then, samples are quenched to a given temperature by free cooling, then timing is started and sample is held for minutes according to experimental requirement. Image is analyzed to determine the time for beginning of crystallization (incubation time).

3. Results and discussion

Fig. 2 shows DTA curves for quenched slags with heating rate of 10K/min . Overall, there are step like transition, two exothermic peaks and two endothermic peaks in all curves. Step-like transitions correspond to glass transition since quenched slags are in amorphous state. Two exothermic peaks reflect two step crystallizations of quenched slags. Solidus temperature and liquidus temperature could be obtained from two endothermic peaks. The onset of the first peak is designated as solidus temperature of sample, while the peak temperature of the second peak is designated as liquidus temperature. Detailed methods for determining solidus and liquidus temperature from DTA measurements could be found in Ref.9. Characteristic temperatures of quenched slag samples were organized in Table 2.

As seen in Table 2, liquidus temperature T_L for quenched samples decrease with increase of B_2O_3 content from 0% to 10%. Due to low melting point, B_2O_3 is regarded as a good flux agent to decrease melting temperature of slag. There

were some reports on the effect of B_2O_3 on breaking temperature or melting temperature of slag. Fox *et al.* [3] found that B_2O_3 decrease breaking temperature of fluoride-free fluxes. Wang *et al.* [10] observed that B_2O_3 decreases melting temperature of ladle slags. There are some differences among breaking temperature, melting temperature and liquidus temperature. Breaking temperature is temperature below which there is a marked increase of viscosity, and determined by viscosity measurement [3]. Melting temperature is defined as the temperature at which the height of flux sample is reduced to one-half of its original height and determined using hemisphere method [10]. Liquidus temperature is temperature where solid sample are fully transformed into liquid. Liquidus temperature is a thermodynamic quantity and could be used to determine the thermodynamic phase diagram of slag. Both breaking temperature and Melting temperature are associated with some kinetics of transformation in heating or cooling process. Accordingly, liquidus temperature determined in the present work could be good thermodynamic references for melting and solidification of slags.

It could be seen from Fig.2 that the crystallization peaks become flat with the increase of B_2O_3 content from sample 1 to 3. The shape of crystallization peaks could indicate the kinetics of crystallization. That shapes of peaks become flat means that crystallization rates become slower. Therefore, the present results indicate that the crystallization process of quenched slag become sluggish with introduction of B_2O_3 . This effect of B_2O_3 on crystallization will be clearly observed in SHTT measurements of the present work, and will be discussed there in detail.

Crystallization products are determined by XRD analysis. Fig.3 shows the XRD patterns for slag samples after heat treated at crystallization peak temperature T_x for 2 hours. The phases were distinguished according to refraction peaks with the help of ICDD cards and marked in XRD patterns. It could be seen from the figure that there are three kinds of crystallization products for treated samples, although there are only two crystallization peaks could be distinguished in DTA curves. The crystallization products are wollastonites ($CaSiO_3$), gehlenite ($Ca_2Al_2SiO_7$) and perovskite ($CaTiO_3$). It is also interesting to observe that wollastonites are only found in samples with B_2O_3 and their amounts increase with the content of B_2O_3 . The reason for effect of B_2O_3 on precipitation of wollastonites remains unclear. The amounts of perovskite increase with increase of TiO_2 content.

SHTT experiments were performed on samples 1-5. All samples were melted at $1300^\circ C$ for several minutes. Sometimes, big bubbles which could be attributed to moisture in samples were found in samples and they were very different to remove. It was found that it is possible to quench all samples except sample 1 to temperature as low as $800^\circ C$ with the largest cooling rate. All sample investigated in the present work are transparent at molten state, which guarantees clear observation of crystal.

TTT diagrams for samples are constructed and shown in Fig.4 and Fig.5 All TTT diagrams are classic C-shaped curves. Only one nose was determined in diagrams, though three different crystals were found in annealed sample for XRD measurements. The crystallization process for sample 3 is very sluggish so that incubation time at investigated temperatures is more than 1000 seconds, therefore no exact incubation time is determined for sample 3. Since crystallization process for sample 1 is so fast that it is impossible to quench the liquid slag into glassy state to temperature lower than $1000^\circ C$, only TTT diagram at temperature more than $1000^\circ C$ were determined at the present

work.

As shown in Fig.4, addition of B_2O_3 significantly increases the incubation time of crystallization for slag samples, which means that B_2O_3 could decrease crystallization ability of slags. Slag with 0% B_2O_3 has a minimum incubation time less than 1 second at nose temperature, while slag with 10% B_2O_3 was not found to be crystallized within 1000 seconds.

The effect of B_2O_3 on crystalline fraction in solid slags was previously investigated by Chang et al.[11] They found the crystalline fraction will be decreased if F in slag is replaced by B_2O_3 . Fox et al. [3]also investigated the crystallization of fluoride-free mould fluxes with Na_2O and B_2O_3 . They obtained a slag film with 52% crystallinity for flux with 1.5% B_2O_3 and a completely glassy film for flux with 5%. The present result for B_2O_3 effect is consistent with these reports.

B_2O_3 is generally accepted as a network forming oxide in slags[12]. Complex networks based on $[BO_3]$ triangular unit and $[BO_4]$ tetrahedral unit could form in structure of slags containing B_2O_3 . In borosilicate slags, borate network could also incorporate into silicate network to increase the complexity of network structure[13]. Increased complexity of network structure helps to improve the glass forming ability of molten slag and weaken the crystallization ability of slag. Therefore, B_2O_3 is also regarded as a good glass forming oxide. It was reported that [3] there was no break temperature found in viscosity temperature curves in slag with more than 8% B_2O_3 content. This indicates that no crystal formed during cooling in viscosity measurements and slag become glassy.

Effect of TiO_2 on the crystallization of slag samples is not as obvious as that of B_2O_3 . It might be due to uncertainty for TTT diagram determined by SHTT technique. For example, the first crystal is judged by eyes of investigator. As shown in Fig.6, Incubation time at nose temperature change slightly as TiO_2 content increase from 3% to 5%, and then decrease as TiO_2 content increase from 5% to 10%. It seems that crystallization of slag is promoted as TiO_2 increase from 5% to 10%. It has been reported that increase of TiO_2 in slag would lead to decrease of viscosity of slag [14,15]. Low viscosity of slag is favorable to crystallization of slag with lower barrier for diffusion. Accordingly, increase of TiO_2 in slag would promote crystallization ability of slags.

Morphologies of crystallization products could be easily observed with the help of camera in SHTT device. A gradually change of morphology from high temperature to lower temperature was clearly found in Fig.6. At low temperature (900°C), a lot of small crystals developed and sample quickly lost transparency due to “clouds” made by these crystals. At 925°C and 1000°C, needle-like crystals appeared at bulk sample and grew longer quickly. These needle-like crystals interweaved and made samples opaque. At 1025°C, facet crystals were observed at any place of sample. At 1050°C, columnar crystals appeared from edge of sample and developed towards center of sample. At 1100°C, large equiaxed dendrites formed from edge or the center of sample.

Morphologies of crystals produced in SHTT device have also been investigated by some researchers[16-17]. Orrling et al. [16] classified different morphologies observed into different types as follows: Equiaxed crystal at high temperature, columnar crystals from thermocouple towards center, faceted crystals and fine crystals. Kölbl et al. also observed similar morphologies during SHTT measurements. In the present work, all morphologies classified by Orrling

et al have been observed. Furthermore, there is one kind of new morphology as needle-like crystals found in the present work. It is noted in the present work that solidus temperature could be also useful in classification of different morphology. Below solidus temperature, fine, needle-like or single faceted crystal tends to precipitate at any place of sample, while above solidus temperature, columnar or equiaxed dendrites could form from edge or center of sample.

Different morphologies at different temperature were also explained by Kölbl et al [] using the ratio of the growth to nucleation rate. Big dendrites form at high temperature with a high ratio of growth to nucleation rate. Fine crystal form at lower temperature with low ratio of growth to nucleation rate and Bulk nucleation takes place. During the present investigation, homogeneous nucleation of crystal is difficult at high temperature since small supercooling degree leads to low thermodynamic driving force. Heterogeneous nucleation tends to take place on the edge of sample with thermocouple as nucleation sites. Due to low viscosity at high temperature, growth of crystal is fast and leads to development of columnar crystal towards center. Bubbles in sample could be also another source for nucleation site, which leads to development of dendrites in the center of sample. In contrast, bulk crystallization could take place at lower temperature due to higher driving force. High viscosity of supercooled liquid is a barrier for growth of crystal. Growth of small crystal is inhibited and cloud of fine crystal forms.

Table 2 Characteristic temperatures of slag samples determined by DTA (unit in °C)

Sample No.	T_g	T_{x1}	T_{x2}	T_s	T_L
1 ($B_2O_3\%=0, TiO_2\%=5$)	713	935	1054	1099	1165
2 ($B_2O_3\%=5, TiO_2\%=5$)	707	770	886	1032	1119
3 ($B_2O_3\%=10, TiO_2\%=5$)	586	672	818	887	930
4 ($B_2O_3\%=5, TiO_2\%=10$)	704	787	891	1004	1115

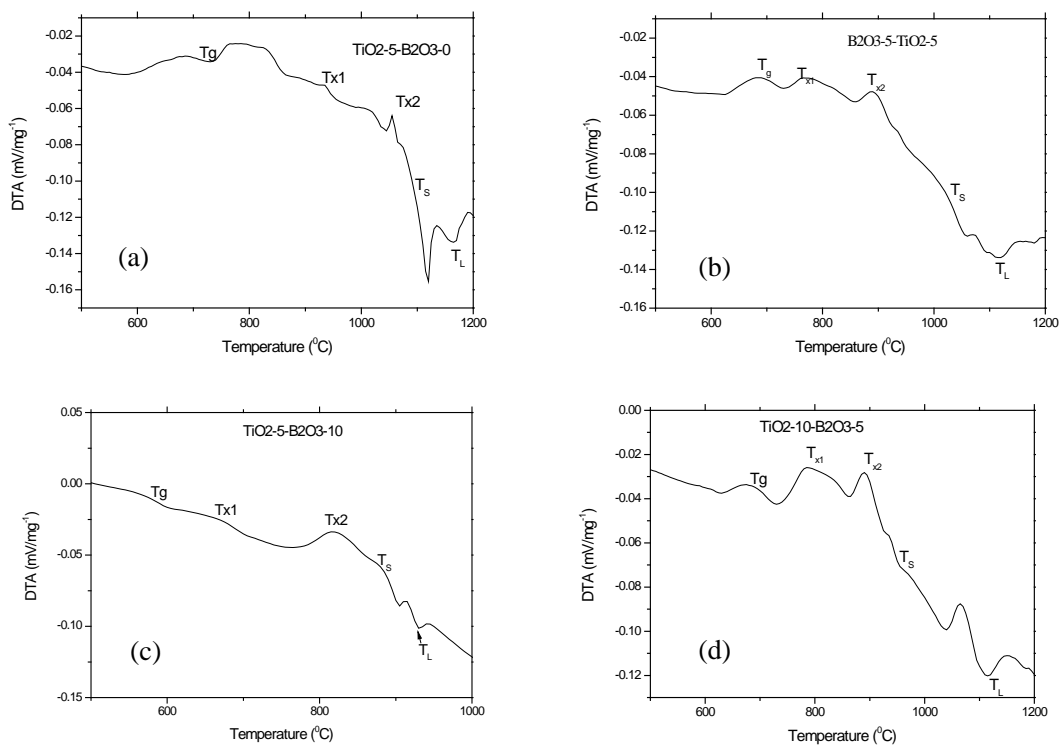


Fig. 2 DTA results for quenched slags (heating rate of 10K/min) (a) sample 1 (b) sample 2 (c) sample 3 (d) sample 4

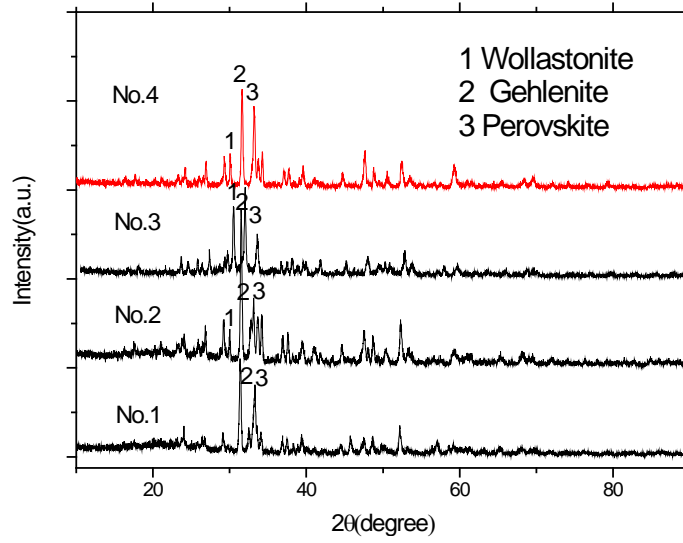


Fig. 3 XRD pattern for slag samples after heated.

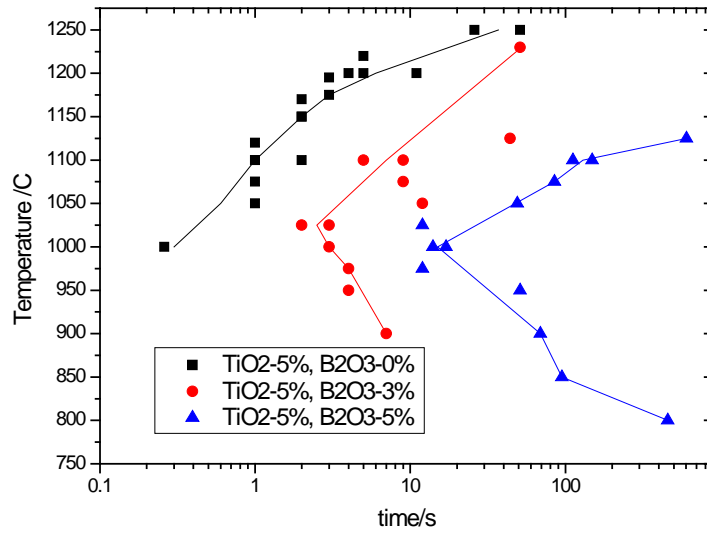


Fig.4 TTT diagrams for sample 1, 2 and 5

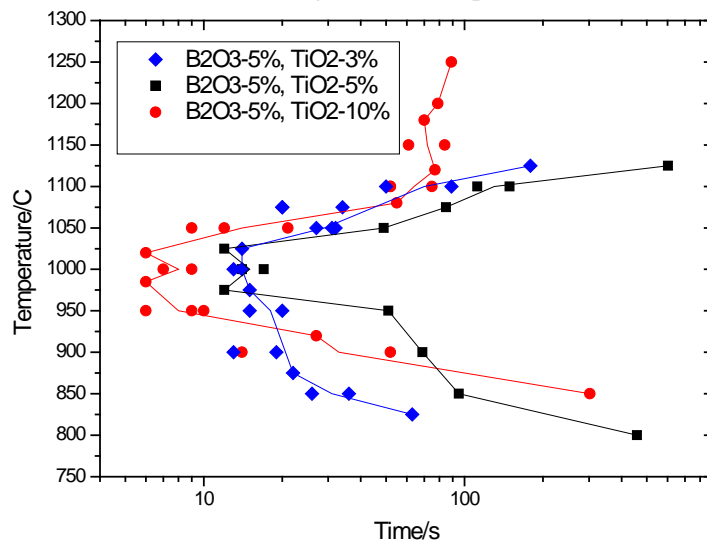


Fig.5 TTT diagrams for sample 2, 4 and 6

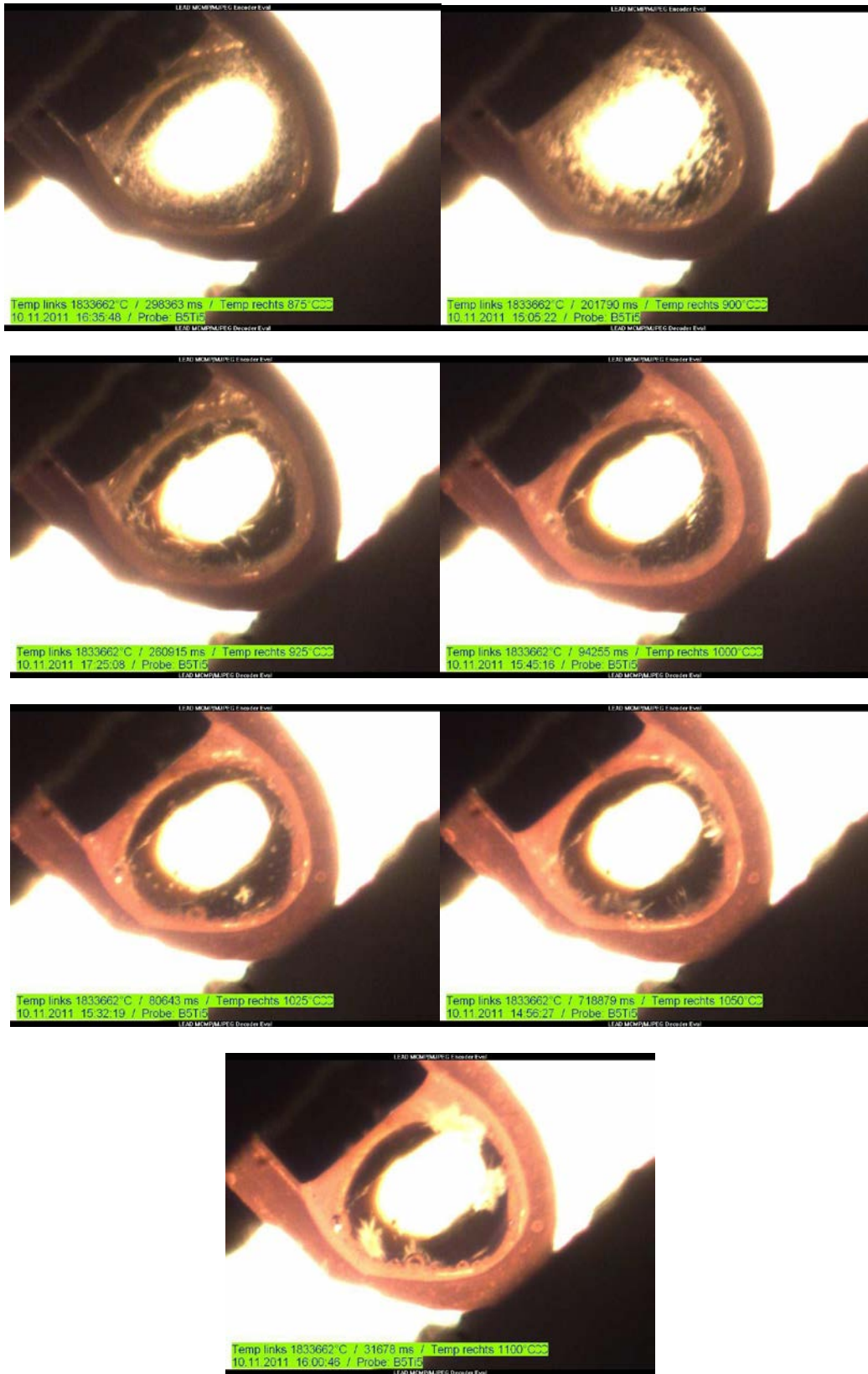


Fig. 6 Images for crystal morphologies investigated at different temperature for sample 2

4. Conclusion

Crystallization behaviors of some slags in $\text{Al}_2\text{O}_3\text{-CaO-MgO-Na}_2\text{O-SiO}_2\text{-B}_2\text{O}_3\text{-TiO}_2$ system at fixed $w(\text{CaO})/w(\text{SiO}_2)$ ratio were investigated using Single Hot Thermocouple Technique (SHTT), Differential Thermal Analysis (DTA) and X-ray diffraction (XRD) technique. Following conclusions could be reached:

1. Liquidus temperature of slags in $\text{Al}_2\text{O}_3\text{-CaO-MgO-Na}_2\text{O-SiO}_2\text{-B}_2\text{O}_3\text{-TiO}_2$ system decreases with increase of B_2O_3 content.
2. Wollastonites (CaSiO_3), gehlenite ($\text{Ca}_2\text{Al}_2\text{SiO}_7$) and perovskite (CaTiO_3) were observed as crystallization products.
3. B_2O_3 can significantly increase the incubation time for crystallization of slags.
4. There are five morphologies for crystals observed at different temperature. From high temperature to lower temperature, crystal shape change from equiaxed crystal, columnar crystal, faceted crystal, needle-like crystal to small crystal "clouds".

Reference

- [1] K.C. Mills and A. B. Fox. The role of mould fluxes in continuous casting-so simple yet so complex. *ISIJ Inter.*, 2003(10), p1479-1486
- [2] A. I. Zaitsev, A. V. Leites, A. D. Litvina, and B. M. Mogutnov. Investigation of the mould powder volatiles during continuous casting, *Steel Res.*, 1994, 65(9), p368-374
- [3] A. B. Fox, K. C. Mills, and D. Lever, *et al.* Development of fluoride-free fluxes for billet casting, *ISIJ Inter.*, 2005, 45(7), p1051-1058
- [4] H. Nakada, K. Nagata. Crystallization of $\text{CaO-SiO}_2\text{-TiO}_2$ Slag as a Candidate for Fluorine Free Mold Flux [J]. *ISIJ Inter.* 2006, 46 (3), p441.
- [5] G. H. Wen, S. Sridhar, P. Tang, X. Qi, Y.Q. Liu. Development of Fluoride-free Mold Powders for Peritectic Steel Slab Casting [J]. *ISIJ Inter.*, 2007, 47 (8), p1117.
- [6] Y. Kashiwaya. Development of Double and Single Hot Thermocouple Technique for in Situ Observation and Measurement of Mold Slag Crystallization. *ISIJ Inter.*, 1998. **38**(4).
- [7] Y. Kashiwaya, C.E. Cicutti, and A.W. Cramb. An Investigation of the Crystallization of a Continuous Casting Mold Slag using the Single Hot Thermocouple Technique[J]. *ISIJ Inter.*, 1998. **38**(4).
- [8] S. Lachmann, and P.R. Scheller. Effect of Al_2O_3 and CaF_2 on the Solidification of Mould Slags and the Heat Transfer through Slag Films, in VIII International Conference on Molten Slags, Fluxes and Salts. 2009: Santiago, pp. 1101.
- [9] J. -C. Zhao (Editor). Method for Phase Diagram Determination, 180-191; 2007, Amsterdam, Elsevier.
- [10] H.M.Wang, T.W.Zhang, H.Zhu, G.R.Li, Y.Q.Yan, and J.H.Wang. Effect of B_2O_3 on Melting Temperature, Viscosity and Desulfurization Capacity of CaO -based Refining Flux, *ISIJ Inter.*, 51(5), 702
- [11] S. H. Chang, and I. J. Lee. Proceedings of continuous casting of steel in developing countries, Beijing, China, 1993, p.832.
- [12] F. D. Richardson. Physical chemistry of melts in metallurgy, Academic Press, London, 1974. vol.I.
- [13] Z. Wang, Q. F. Shu and K. C. Chou. Structure of $\text{CaO-B}_2\text{O}_3\text{-SiO}_2\text{-TiO}_2$ Glasses: a Raman Spectral Study, *ISIJ*

Inter, 2011, 51(7), p.1021-1027

- [14] V. H. Schenck, and M. G. Froberg. Viskositätsmessungen an flüssigen schlacken des systems CaO-SiO₂-TiO₂ im Temperaturbereich von 1300 bis 1600°C, Arch. Eisenhüttenwesen, 1962, p421-425
- [15] K. C. Mills. Viscosities of molten slags, In Slag Atlas [M], 2nd Edition, Edited by Verein Deutscher Eisenheuttenleute (VDEh), Verlag Stahleisen GmbH, 1995, p.354, p.357
- [16] C. Orrling, S. Sridar, and A. W. Cramb. In situ observations and thermal analysis of crystallization phenomena in mold slags, High Temperature Materials and processes, 2001, 20(3-4), p.195-199.
- [17] N. Kölbl, I. Marschal, and H. Harmuth. Single hot thermocouple technique for the characterization of the crystallization behavior of transparent or translucent liquids, J. Mater. Sci., 46. p.6248-6254